The Effects of Silver Ion Implantation on Structural and Morphological Performance of Hydroxyapatite Coatings

K. Suchanek[a,*], D. Sobol[a], M. Mitura-Nowak[b], M. Perzanowski[b] and M. Marszałek[b]

[a]Institute of Physics, Cracow University of Technology, Podchorążych 1, Kraków, 30-084, Poland
[b]The Institute of Nuclear Physics, Polish Academy of Sciences, E. Radzikowskiego 152, 31-342 Krakow, Poland

Hydroxyapatite coating composed of hexagonal rods are modified with silver ions to improve their antibacterial activity. The coatings are irradiated at room temperature using 15 keV Ag^+ ion source and three different ion doses up to 6×10^{16} ions/cm^2. Morphological and structural changes in the crystal structure of hydroxyapatite are followed as a function of Ag^+ ion dose using scanning electron microscopy, energy dispersive X-ray spectroscopy, X-ray diffraction, and the Raman spectroscopy. We observed that implantation did not produce any morphological changes in crystals. Based on the X-ray diffraction data, we show that lattice constant of hydroxyapatite remains unchanged for all samples irrespective of the Ag^+ ion dose. However, ion-induced defects formation is evidenced by detailed X-ray diffraction line profile analysis and broadening of the diffraction maxima with increasing Ag^+ ion dose.

1. Introduction

Recently, there is a great demand for novel biomaterials, to use as orthopedic implants, to repair bone defects caused by trauma, disease, or genetic disorders. Hydroxyapatite (HAp, $Ca_{10}(PO_4)_6(OH)_2$) is widely used in the field because its chemical composition resembles that of the bone, it promotes the desired tissue response, and accelerates bone growth around the implant [1, 2]. HAp has excellent biocompatibility and exhibits bioactive properties, i.e., it bonds directly to the host bone without the formation of fibrous tissue at the interface [3]. However, to avoid the development of infections after implantation, an important issue remains that is the need to ameliorate the inflammatory response elicited by replacement surgery in order to facilitate regeneration following trauma. Hence arises the idea to develop functional materials with good osteoinductivity and adequate internal antibacterial protection at the same time.

Silver (Ag) is a natural antibacterial agent that has strong activity against a broad spectrum of bacteria, including those resistant to antibiotics [4, 5]. Enriching hydroxyapatite with silver nanoparticles has become a fairly common method of improving the bactericidal properties of biomaterials [6, 7]. However, a release of high concentration of Ag nanoparticles can potentially cause high cytotoxicity [8, 9]. In view of this, the ion implantation method limiting the mobility of Ag^+ ions can become an effective way to improve the overall performance of HAp/Ag systems.

Ion implantation technique is a promising physical method that enables to introduce a wide range of atomic species into surface region of solid material [10]. It is a doping method in which high energy ions penetrate into the substrate while losing energy due to inelastic and elastic collisions with the target atoms. Finally, the ions come to rest and occupy a certain lattice site within the crystal structure. Compared with other methods ion implantation possesses unique advantages including precise control of the dopant concentration and the purity of the implanted species [11]. However, the collisional cascade may result in the production of radiation defects in the crystal structure and for sufficiently high doses may lead to the phase transformation of the irradiated surface. These changes may affect the properties of HAp crystals, in particular mechanical properties [12] and the *in vivo* biological response [11].

In the present study, HAp coatings doped with silver ions were prepared through two step process. Hydroxyapatite coatings were fabricated on titanium substrate by hydrothermal synthesis from aqueous solution and subsequently doped with silver through ion implantation method. We provide detailed investigation of those composite systems to get the knowledge of the effects of ion irradiation on their structural and morphological performance.

2. Material and methods

2.1. HAp/Ag coatings fabrication

The hydroxyapatite coatings were formed on the surface of Ti substrates through the hydrothermal reaction in aqueous solution containing calcium nitrate $Ca(NO_3)_2$, diammonium phosphate $(NH_4)_2HPO_4$,

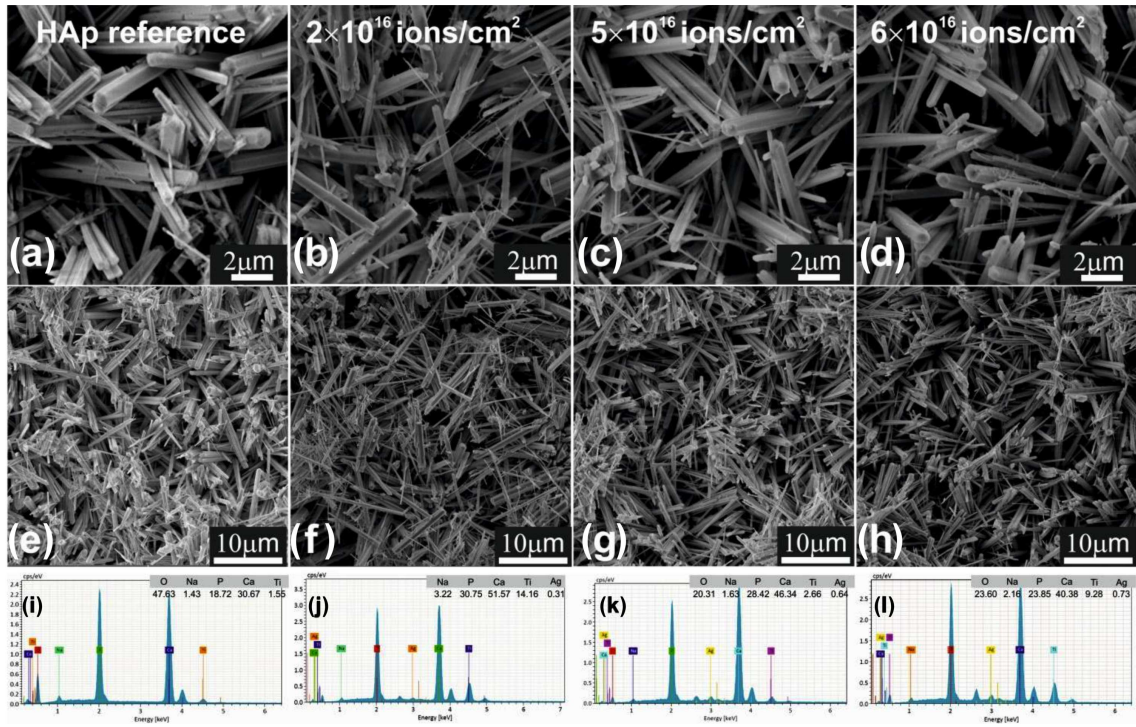*corresponding author; e-mail:
katarzyna.suchanek@pk.edu.pl

Fig. 1. The morphological and elemental analysis of HAp coatings. (a–d) Low and (e–h) high magnification SEM images of the surface before and after Ag$^+$ ion implantation. (a,e) As-prepared HAp and HAp implanted with (b,f) 2×10^{16} ions/cm^{-2}, (c,g) 5×10^{16} ions/cm^{-2} and (d,h) 6×10^{16} ions/cm^{-2} of ions dose, respectively. Parts (i–l) show the EDS spectrographs of all synthesized specimens.

ethylenediamine tetraacetic acid (EDTA), and monoethanoloamine (MEA) as described in detail elsewhere [13]. The final pH of the reaction solution was equal to 10.0. The mixture was autoclaved in hydrothermal reactor (Carl Roth 2098.1) for 7 h at 200 °C. The HAp coatings were subsequently implanted with silver ions Ag$^+$ using an ion implantation method [14]. The acceleration energy and typical ion beam current density were 15 keV and 1 μA/cm^2, respectively. The implantation chamber pressure was 1×10^{-6} Pa. The projected range of Ag$^+$ in Ca$_{10}$(PO$_4$)$_6$(OH)$_2$ was calculated using the SRIM code [15] and the average depth of Ag$^+$ ions was about 25 nm. To determine the influence of ion implantation on physicochemical properties of HAp crystals three ion doses were selected: 2×10^{16}, 5×10^{16}, 6×10^{16} ions/cm^2.

2.2. Surface characterization

The morphological and structural properties of all specimens were characterized by scanning electron microscopy (SEM), energy dispersive X-ray spectroscopy (EDS), X-ray diffraction (XRD), and the Raman spectroscopy. The surface morphology of the as-deposited HAp coatings was examined using scanning electron microscope (SEM, Tescan Vega 3). The elemental analysis was performed using EDS spectrometer (QUANTAX EDS, Bruker) equipped with an XFlash 610M detector with the resolution of < 129 eV for

the Mn K_α line. The XRD measurements were carried out with PANalytical X'Pert Pro diffractometer using the standard θ–2θ geometry. The patterns were taken using Cu K_α ($\lambda = 1.54$ Å) radiation operating at 30 mA and 40 kV. The angular resolution of the instrument was calibrated using LaB$_6$ line profile standard (SRM660a-NIST certificate). X-ray diffraction patterns were taken over the 2θ range of 20°–60° with a 0.05° step size. The chemical composition of the HAp coatings was determined with the Raman spectrometer (Almega XR of Thermo Electron Corp.). A 532 nm laser was used to excite the Raman signal. The data were recorded in the spectral range from 100 cm^{-1} to 4000 cm^{-1} with spectral resolution of 2 cm^{-1}.

3. Results and discussion

The HAp coatings synthesized during the hydrothermal process were subjected to ion implantation in three doses of 2×10^{16}, 5×10^{16}, and 6×10^{16} ions/cm^2. In Fig. 1 we show SEM images of HAp coatings before and after ion implantation. The SEM images of HAp prior to implantation show crystals composed of hexagonal rods with micrometer sizes (Fig. 1a, e). The SEM analysis of HAp surface after Ag$^+$ ion irradiation demonstrates that implantation did not produce any morphological changes in crystals, such as cracking, crushing, or melting (Fig. 1b–d, f–h). For all doses of Ag$^+$ ions,

the HAp morphology remains unchanged. The samples were also analysed using EDS spectroscopy to evaluate their chemical composition (Fig. 1i–l). The results confirm the presence of Ca and P as a main component of hydroxyapatite phase. In addition, the analysis of implanted specimens indicates the presence of silver and its content increases with the implantation dose. Trace amounts of sodium and titanium observed in EDS spectrum originate from the reagent used during hydrothermal reaction and titanium substrate, respectively.

The phase composition of HAp coatings with different Ag^+ ion concentration was investigated by XRD method, as shown in Fig. 2. The spectra of all samples are dominated by the diffraction peaks originated from pure HAp phase with the space group $P63/m$ (ICSD-PDF #00-009-0432). We also observed α-Ti and crystalline TiO_2 with the tetragonal rutile structure, originating from the substrate. We do not observe any additional phases of other calcium phosphates or compounds such as silver oxide or silver phosphate.

As was mentioned above, the main disadvantage of ion implantation is the generation of damage in the crystal structure. These may be in the form of point defects, such as vacancies or interstitials. By calculating the cell parameters of pure and Ag-implanted HAp crystals, it was found that a and c lattice constants remain unchanged for all samples irrespective of the Ag^+ ions dose and are equal to: $a = 9.77$ Å and $c = 6.89$ Å. The ionic radius of Ag^+ (1.15 Å) is comparable with that of Ca^{2+} (1.00 Å). Hence if Ag^+ ion is incorporated into the crystal structure, there is no lattice mismatch and therefore no lattice constant distortion. In the next step in order to accurately follow the strain evolution during the implantation, we made a complementary view of the damage created by silver ions, by XRD peak profile analysis. Analysis of the XRD line profile is important because deviations from the ideal crystallinity lead to its broadening [16, 17]. The main sources of the spectral line broadening are the finite size of crystallites or the deformations of the crystal, resulting from the formation of defects. The fit of individual Bragg lines has been performed using pseudo-Voigt function and the peak widths were determined as FWHM. Five peaks were selected for analysis, which appear at the diffraction angle of 25.91°, 31.74°, 32.84°, 34.05°, and 46.63° and correspond to (002), (211), (300), (202), and (222) reflection planes, respectively.

Figure 3 shows results determined from the above analysis. According to the data obtained, the full width at half maximum of the individual Bragg line increases with increasing ion dose in all cases. The magnitude of distortion is most prominent for sample irradiated with Ag^+ ion dose of 6×10^{16} ions/cm². The change in crystallographic characteristics is due to appearance of defects in HAp structure.

The Raman spectroscopy provides additional insight into the structural properties of synthesised materials. Figure 4 shows the Raman spectra of HAp coatings
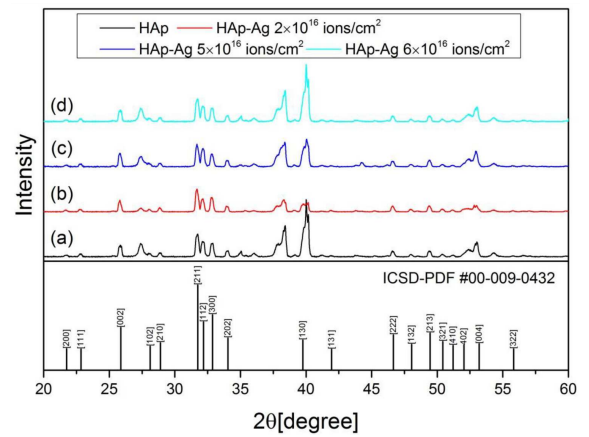

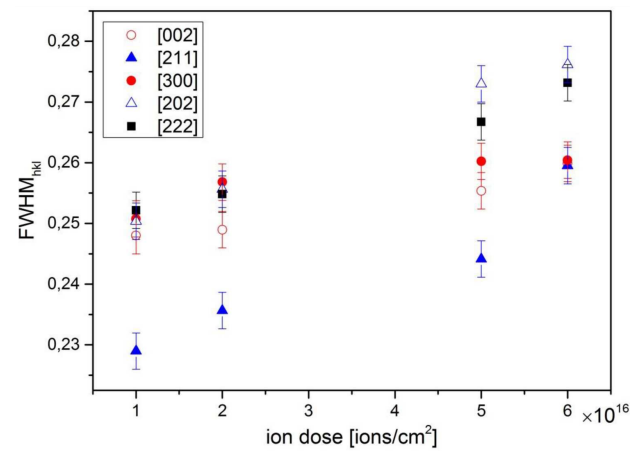Fig. 2. XRD patterns of hydrothermally synthesized HAp coatings (a) prior and (b–d) after Ag^+ ion implantation.

Fig. 3. Dependence of FWHM of individual Bragg lines on Ag^+ ions dose.

investigated in this study. The Raman spectrum of HAp prior to implantation is characterized by peaks at 420–450 cm⁻¹, 580–600 cm⁻¹, 940–970 cm⁻¹, and 1040–1070 cm⁻¹ which are attributed to doubly degenerate O–P–O bending mode ($\nu2$), triply degenerate O–P–O bending mode ($\nu4$), non-degenerate symmetric stretching P–O mode ($\nu1$), and triply degenerate asymmetric P–O stretching mode ($\nu3$), respectively [18, 19]. The band representing OH^- symmetric stretching vibration is observed in the high wave-number region at 3575 cm⁻¹. Implantation with the Ag^+ ion dose up to 5×10^{16} ions/cm² does not cause any variations in peak position and width. Then for 6×10^{16} ions/cm² complete disappearance of peak related to OH^- vibration takes place along with a decrease in the peak intensity at 420–450 cm⁻¹, 580–600 cm⁻¹, and 1040–1070 cm⁻¹. Moreover, the Raman peak at 960 cm⁻¹ decreases, broadens, and shifts toward lower wave numbers. This indicates that for Ag^+ ion dose of 6×10^{16} ions/cm²
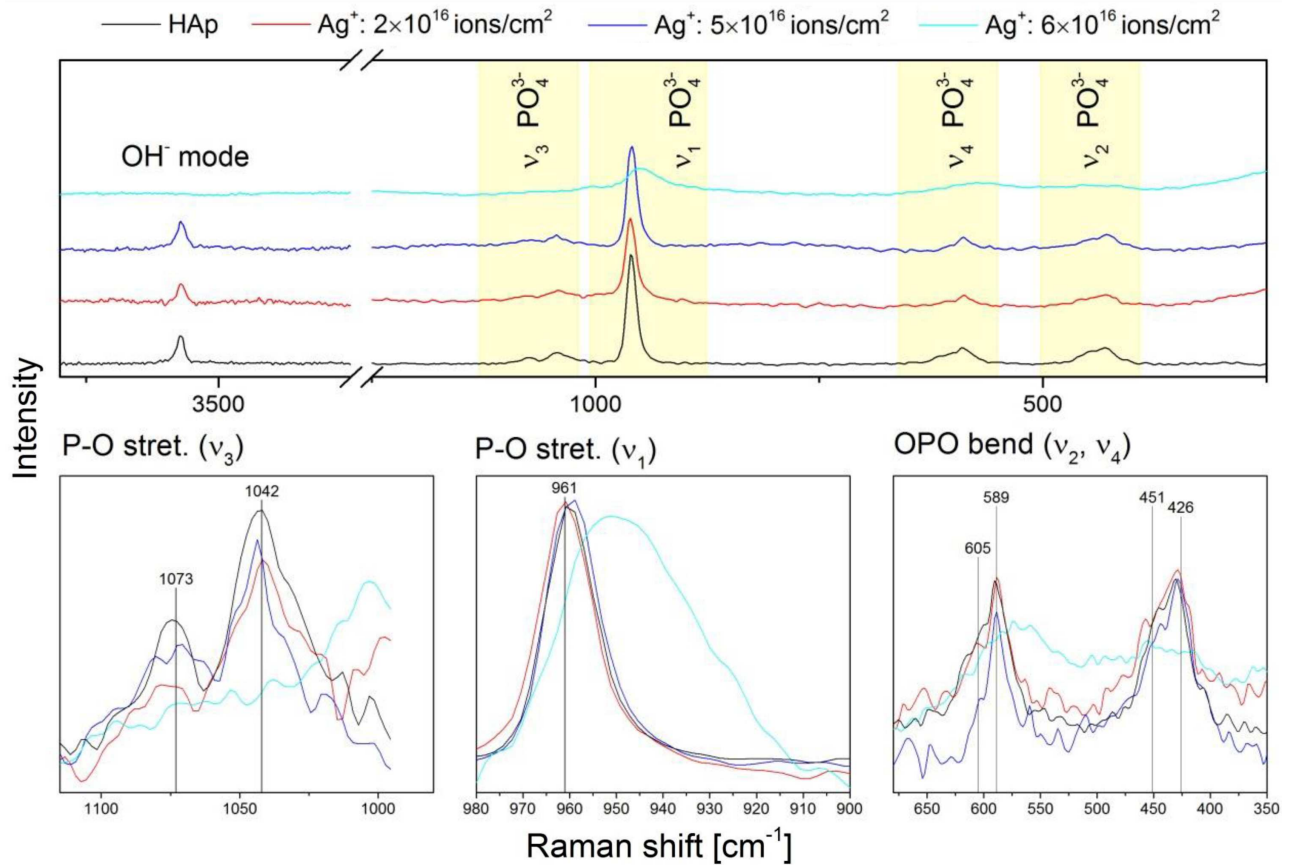
Fig. 4. The Raman spectra of HAp coatings before and after ion implantation along with a detailed inspection of the spectral range of phosphate bands in the frequency range of 350–1100 cm^{-1}.

the chemical bonds in the hydroxyapatite structure are broken because of the irradiation effect. This result is consistent with the data obtained from the XRD investigation, but indicates that the latter method is more sensitive to the structural changes induced by the ion implantation of the hydroxyapatite crystals.

4. Conclusion

In the present study, HAp coatings synthesized under hydrothermal condition were implanted with silver ions with different doses ranging from 2 to 6×10^{16} ions/cm^2. The effect of Ag$^+$ implantation on morphological and structural performance of crystals was investigated. Notably, the Ag$^+$ ion implantation, within the range of doses used, did not change the morphological properties of HAp crystals. The overall XRD patterns of implanted HAp were found to be nearly identical to this obtained for HAp before irradiation. However, a detailed inspection of XRD peak profile reveals that as a result of Ag$^+$ ion irradiation the FWHM of the individual Bragg line linearly increases with ion dose used. The changes in crystallographic characteristics indicate the formation of defects in HAp structure. Implantation of Ag$^+$ with an implantation dose of 6×10^{16} ions/cm^2

decreases the intensity of all characteristic Raman bands. Although implantation leads to changes in the structure of hydroxyapatite, they are not significant. This suggests that Ag-implanted HAp coatings have a great potential for bone implants providing intrinsic bacterial resistance.

References

[1] M.J. Olszta, X. Cheng, S.S. Jee, R. Kumar, Y.Y. Kim, M.J. Kaufman, E.P. Douglas, L.B. Gower, *Mater. Sci. Eng. R* **58**, 77 (2007).

[2] N. Eliaz, N. Metoki, *Materials* **10**, 334 (2017).

[3] S.V. Dorozhkin, *Mater. Sci. Eng. C* **55**, 272 (2015).

[4] K. Zheng, M.I. Setyawati, D. Tai Leong, J. Xie, *Coordin. Chem. Rev.* **357**, 1 (2018).

[5] C. Marambio-Jones, E.M. Hoek, *J. Nanopart. Res.* **12**, 1531 (2010).

[6] M. Vukomanović, U. Repnik, T. Zavašnik-Bergant, R. Kostanjšek, S.D. Škapin, D. Suvorov, *ACS Biomater. Sci. Eng.* **1**, 935 (2015).

[7] M. Li, X. Liu, Z. Xu, K.W.K. Yeung, S. Wu, *ACS Appl. Mater. Interfaces* **8**, 33972 (2016).

[8] X. Chen, H.J. Schluesener, *Toxicol. Lett.* **176**, 1 (2008).

[9] S.W.P. Wijnhoven, W.J.G.M. Peijnenburg, C.A. Herberts, et al., *Nanotoxicology* **3**, 109 (2009).

[10] J.S. Williams, J.M. Poate, in: *Ion Implantation and Beam Processing*, Eds. J.S. Williams, J.M. Poate, Academic Press, 1984, p. 1.

[11] T.R. Rautray, R. Narayanan, K.H. Kim, *Prog. Mater. Sci.* **56**, 1137 (2011).

[12] A. Zamiri, S. De, *J. Mech. Behav. Biomed. Mater.* **4**, 146 (2011).

[13] K. Suchanek, M. Perzanowski, K. Suchy, M. Lekka, B. Szaraniec, M. Marszałek, *Surf. Coat. Technol.* **364**, 298 (2019).

[14] B. Rajchel, M. Drwiega, E. Lipińska, M. Wierba, *Nucl. Instrum. Methods Phys. Res. B* **89**, 342 (1994).

[15] J.F. Ziegler, SRIM, www.srim.org.

[16] K. Venkateswarlu, A. Chandra Bose, N. Rameshbabu, *Physica B* **405**, 4256 (2010).

[17] P. Scardi, M. Leoni, *Acta Crystallogr. A* **57**, 604 (2001).

[18] R. Cusco, F. Guitian, S. de Aza, L. Artus, *J. Eur. Ceram. Soc.* **18**, 1301 (1998).

[19] H. Tsuda, J. Arends, *J. Dent. Res.* **73**, 1703 (1994).